Journal of Trace Elements in Medicine and Biology 55 (2019) 127–135

Contents lists available at ScienceDirect

Journal of Trace Elements in Medicine and Biology

journal homepage: www.elsevier.com/locate/jtemb

Bioinorganic chemistry

Dose-response relationships between copper and its biocompatibility/antibacterial activities

Kunqiang Li[a,b], Chao Xia[a,b], Yuqin Qiao[a,*], Xuanyong Liu[a,b,*]

[a] State Key Laboratory of High Performance Ceramics and Superfine Microstructure, Shanghai Institute of Ceramics, Chinese Academy of Sciences, Shanghai 200050, China

[b] Center of Materials Science and Optoelectronics Engineering, University of Chinese Academy of Sciences, Beijing 100049, China

ARTICLE INFO

Keywords:
Copper
Antibacterial
Osteogenesis
Angiogenesis
Dose-response relationship

ABSTRACT

Background: Copper has already been widely used in the modification of biomaterials because it possesses multifunctional biological effects like osteogenic, angiogenic and antibacterial activities. However, it is still not clear how different cell lines and bacteria will respond to different concentrations of Cu^{2+}, which is very critical to the application of copper-doped implants.

Methods: This study aimed to explore the dose-response relationships of Cu^{2+} and its biological effects *in vitro*. Rat bone marrow mesenchymal stem cell (rBMSCs), mouse osteoblastic cell line (MC3T3-E1), and human umbilical vein endothelial cells (HUVECs) were used to evaluate cellular behaviors. *Staphylococcus aureus* (*S. aureus*) and *Escherichia coli* (*E. coli*) were used to evaluate bacterial behaviors.

Results: Results showed that the HUVECs exhibited significantly higher tolerance to copper ions than MC3T3-E1 and rBMSCs. The IC_{50} values of copper for HUVECs, MC3T3-E1 and HUVECs were approximated to 327.9 μM, 134.6 μM, and 0.7 μM, respectively. Besides, the threshold concentration of copper for effective inhibition against bacteria growth is 37 μM. When the concentration exceeded the threshold value, antibacterial activity could increase dramatically.

Conclusions: These results altogether establish a technological foundation for the application of copper-doped biomaterials in bone growth and remodeling.

1. Introduction

Nowadays, orthopedic and dental implants are considered to be reconstructive treatments for bone or tooth replacements. Although there has been a great progress in their clinical success rates, failures continue to occur. Inadequate integration and bacterial infections are generally believed to be the main factors for implant failures [1]. Therefore, implanted biomaterials were required to possess multifunctionalities to promote the bone remodeling process and prevent bacterial infections [2,3]. At present, many physical and chemical methods were used for modifications of materials to improve their bioactivities. One of the most effective modification methods is doping essential elements such as zinc [4,5], calcium [6,7], manganese [8], and copper [9–12] into biomaterials. Recent studies have provided strong evidences for the involvement of these elements in bone metabolism, while excessive amounts of released ions could lead to cytotoxicity. Hence, the dose-response relationships between elements and their biological effects should be explored to avoid adverse effects.

Increasing evidence in the literature indicates that angiogenesis and osteogenesis are coupled for bone function and fracture healing [13,14]. Among all essential elements, copper has drawn particular attention for its various fascinating roles in bone formation and possessing antibacterial activity [15]. For example, copper ions have been reported to enhance angiogenesis by stabilizing hypoxia-inducible factor (HIF-1α) and stimulating vascular endothelial growth factor (VEGF) expression [16,17]. Another recent study revealed that HIF-1α signaling in bone-building osteoblasts is central to the coupling of angiogenesis and bone development in mice [18]. Moreover, copper was shown to increase the ability of mesenchymal stem cells (MSCs) to differentiate into osteogenic lineage and can inhibit osteoclast activity [19,20]. These results showed that copper potentially has a positive impact on bone metabolism. Besides, it is well established that copper has demonstrated excellent antimicrobial activities against Gram-positive and Gram-negative bacteria, including methicillin-resistant

* Corresponding authors at: State Key Laboratory of High Performance Ceramics and Superfine Microstructure, Shanghai Institute of Ceramics, Chinese Academy of Sciences, Shanghai 200050, China.

E-mail addresses: qiaoyq@mail.sic.ac.cn (Y. Qiao), xyliu@mail.sic.ac.cn (X. Liu).

https://doi.org/10.1016/j.jtemb.2019.06.015
Received 1 April 2019; Received in revised form 6 June 2019; Accepted 19 June 2019

Staphylococcus aureus (MRSA), vancomycin-resistant enterococci (VRE) and fungi [21,22]. In this context, copper is widely doped to biomaterials such as bio-ceramics [23–25], bio-glasses [10,26,27], metal-organic framework-hydrogel system [28], biomedical titanium alloys [29–34], Mg alloys [35], etc., to endow them with osteogenic, angiogenic and antibacterial activities.

The multiple biological functions of copper are ascribed to its involvement in many aspects of cellular metabolism as a cofactor or activator [36]. Thus, Cu homeostasis is tightly regulated through Cu transporters and metallochaperones [37]. Excess copper may cause metabolic dysfunctions and is associated with severe neurodegenerative diseases [38]. This raises concerns about whether the amount of doped copper might be safe in designing biomaterials. However, there is little information on the dose-response relationship between copper and its biological effects. For instance, Liu et al. prepared Mg-Cu alloys with different contents of copper [35]. The results showed that Mg-0.03Cu could improve the cell viability, osteogenic and angiogenic activities, while these were inhibited by increased amount of copper (Mg-0.57). Wang et al. reported that copper-containing mesoporous bioactive glass (Cu-MBG) showed a dose-dependent cytotoxicity of copper on 3T3 fibroblasts [39]. Guo et al. revealed that 0.05% CCPP (Cu-containing calcium polyphosphate) scaffolds exhibited better cytocompatibility and ability to stimulate osteogenesis and angiogenesis compared to those scaffolds doped with higher amounts of copper (0.1% CCPP, 0.2% CCPP, and 0.5% CCPP) [40]. Although all these *in vitro* experiments have revealed that higher amount of doped copper could compromise its efficiency in promoting biological effects or induce cytotoxicity, they are not directly applicable to copper doping in designing different biomaterials. Because different amounts of copper are generally presented as discrete and scattered data points in these works, which cannot provide a clear trend towards dose-response relationship. Thus, the present study was undertaken to identify a dose-response relationship between copper and its biological effects.

In this work, we systematically studied the dose-response relationship of Cu^{2+} by evaluating the osteogenic, angiogenic, and antibacterial activities. Three kinds of cells, human umbilical vein endothelial cells (HUVECs), mouse osteoblastic cells (MC3T3-E1), and rat bone marrow mesenchymal stem cells (rBMSCs), are chosen to evaluate cellular behaviors. *S. aureus* and *E. coli* are chosen to evaluate antibacterial activity.

2. Material and methods

2.1. Preparation of Cu^{2+} solution

Copper chloride ($CuCl_2{\cdot}2H_2O$, AR) was selected as the copper source. The preparation process of Cu^{2+} solution as follows: $CuCl_2{\cdot}2H_2O$ was dissolved in phosphate buffered saline (PBS) to prepare 100 mM $CuCl_2$ solution, and then the solution was filtered with 0.22 μM filter and stored in refrigerator at 4 °C before using. The solvent of Cu^{2+} solution for bacteria culturing was physiological saline solution. The $CuCl_2$ stock solutions were diluted to a series of concentrations by cell culture medium or physiological saline solution, respectively, for cellular or bacterial experiments.

2.2. Cell culture

HUVECs was cultured in Endothelial Cell Growth Medium (ECM) with 5% fetal bovine serum (FBS), 1% penicillin and streptomycin (ScienCell, CA), and 1% cell growth supplement (CGS) at 37 °C in incubator of 5% CO_2. MC3T3-E1 and rBMSCs were cultured in α-minimum essential medium (α-MEM, Gibco, USA) with 10% FBS (Gibco, USA), 1% penicillin/streptomycin (Gibco, USA). Cell culture medium was replaced with fresh culture medium every 3 days. For cell seeding, the cells were detached from culture plate by culturing with trypsin/EDTA (0.25% trypsin, 0.02% EDTA, Gibco, Invitrogen) solution for 3 min at 37 °C. Then, the detached cells were collected and centrifuged for 5 min at 1000 rpm. Finally, the cells were resuspended with culture medium and seeded in cell plates.

2.3. Cell viability test

Cell viability was assessed by alamarBlue™ (Invitrogen, USA) according to the manufacturer's instructions. Before seeding cells, a series of culture medium with different concentrations of Cu^{2+} were prepared. The concentrations of Cu^{2+} included 0.0056 μM, 0.017 μM, 0.051 μM, 0.15 μM, 0.46 μM, 1.37 μM, 4.12 μM, 12.34 μM, 37 μM, 111 μM, 333 μM, and 1 mM for all three kinds of cells. The other two concentrations (222 μM and 666 μM) were extra added for HUVECs. Three kinds of cells were seeded into 96-well plates with density of 1×10^4 cells/well, respectively. The plates were incubated at 37 °C in an incubator of 5% CO_2 for 24 h. Then culture medium was replaced with fresh culture medium containing different concentrations of Cu^{2+}, and the plates were cultured for another 3 days. At the time point, culture medium was discarded, and fresh culture medium with 10% alamarblue and without Cu^{2+} was introduced and cultured for another 2 h. Finally, Cytation 5 Multi-Mode Reader (Biotek, USA) was used to measured fluorescence intensity of culture medium with wavelength of 560 nm (Ex)/590 nm (Em). Inhibition ratio was calculated according to following formula:

$$\text{Inhibition ratio} = \frac{F_0 - F_{sample}}{F_0 - F_{blank}}$$

F_0 was the fluorescence intensity of culture medium without Cu^{2+} in cell culture.

F_{sample} was fluorescence intensity of culture medium containing Cu^{2+} in cell culture.

F_{blank} was fluorescence intensity of 10% alamarblue solution.

2.4. Cell migration assay

HUVECs were seeded on cover glasses in 24-well plates with a cell density of 2×10^5 cells/well. After monolayer cells had formed on cover glasses, a scratched line was made across cover glass by 200 μL pipette tips. Then, the cells were washed twice by PBS and cultured with fresh culture medium containing different concentrations of Cu^{2+} for another 6 h. After that, cells were fixed with 4% paraformaldehyde, penetrated with 0.1% TritonX-100, and blocked with 1 wt% BSA. Finally, cell's nucleus and cytoskeleton were stained with DAPI and Rhodamine-phalloidin, respectively. The images were taken by an Olympus fluorescence microscope in dark.

2.5. Alkaline phosphatase (ALP) activity assay

rBMSCs was seeded into 24-well plates with cell density of 1×10^4 cells/well. After culturing for 24 h, the culture medium was replaced with fresh culture medium containing different concentrations of Cu^{2+}. Culture medium was replaced every 3 days. For ALP qualitative assay, at each time point, the culture medium was discarded, and the cells were rinsed twice with PBS. Then, the cells were fixed by citrate buffer, and then stained by dye mixed with fast blue RR in dark. Images were taken by fluorescence microscope (Olympus GX 71, Olympus, Japan) under brightness field. For ALP quantitative assay, the cells were lysed by lysis buffer with 1% lgepal CA-630, 10 mM Tris-HCl (pH 7.5), 1 mM $MgCl_2$, and 1% protease inhibitor. After that, the cell lysis buffered solutions were centrifuged, and the supernatant was collected. Finally, the collected supernatant was cultured with *p*-nitrophenyl phosphate and glycine buffer at 37 °C for 30 min. Then stop the reaction by adding 50 μL of 1 M NaOH to each well and measure the absorbance of the reaction solution using Cytation 5 Multi-Mode Reader (Biotek, USA) at 405 nm. The total protein content was determined by Pierce™ BCA Protein Assay Kit according to instructions. The relative ALP activity

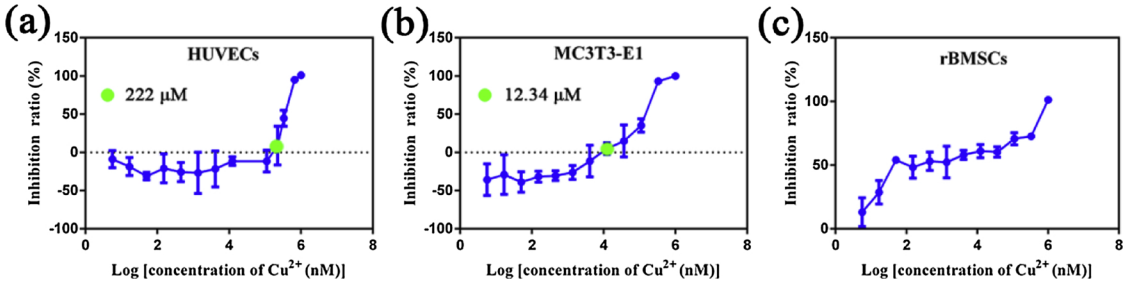

Fig. 1. Inhibition ratio curves of copper ions responses to three kinds of cells: (a) HUVECs, (b) MC3T3-E1, and (c) rBMSCs after culturing for 4 days.

was showed as a ratio of ALP value divided by total protein content.

2.6. Intracellular ROS levels

DCFH-DA (sigma, USA) was chosen to assay Intracellular reactive oxygen content. DCFH-DA could pass through cell membrane and hydrolyzed by esterase into DCFH. The ROS in cell could oxidize DCFH into DCF which could show fluorescence with wavelength of 488 (Ex)/525 (Em). Three kinds of cells were seed into 96-well with a density of 1×10^4 cells/well, respectively. After culturing 1 day, the old culture medium was replaced with new culture medium with different concentrations of Cu^{2+} solution and culturing for another 24 h. Then the cells were orderly stained by DCFH-DA solution and DAPI solution. Finally, fluorescence intensity of DCF and DAPI was measured by Cytation 5 Multi-Mode Reader with wavelength of 360 nm (Ex)/460 nm (Em) for DAPI and 488 nm (Ex)/525 nm (Em) for DCF. The ratio of fluorescence intensity of DCF/fluorescence intensity of DAPI was representative ROS levels.

2.7. Antibacterial activity assay

Staphylococcus aureus (*S. aureus*, ATCC 25923) and *Escherichia coli* (*E. coli*, ATCC 25922) were chosen to assess antibacterial activity of Cu^{2+} by bacterial colony counting method and SEM morphology observation. The preparation of a series of Cu-containing solutions is mentioned above. The concentrations of Cu^{2+} included S1 (0.017 μM), S2 (0.05 μM), S3 (0.15 μM), S4 (0.45 μM), S5 (1.37 μM), S6 (4.12 μM), S7 (12.34 μM), S8 (37 μM), S9 (111 μM), S10 (333 μM), and S11 (1 mM), respectively. The S0 was represented as saline without Cu^{2+}. The procedures of seeding bacteria as follows: 100 μL of bacterial solution at a concentration of 1×10^7 cfu/mL was added into 15 mL centrifuge tubes with 5 mL of different copper-containing saline solutions. After brief vortex-mixing, 60 μL of bacterial solutions for each copper concentration was introduced onto cover glasses in 24-well plates. Then all 15 mL centrifuge tubes and 24-well plates were incubated at 37 °C. After culturing for 12 h, the bacteria on cover glasses in 24-well plates were fixed with 2.5% glutaraldehyde (Gibco, USA)

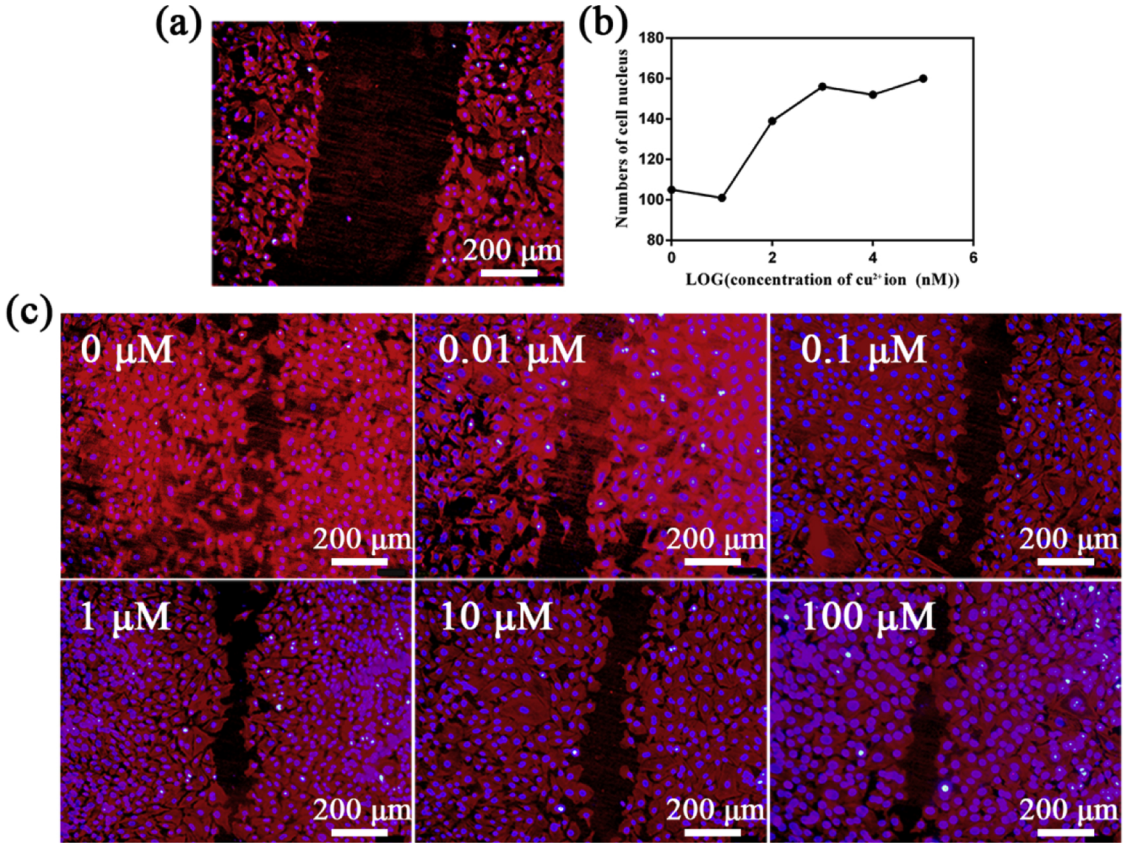

Fig. 2. Image of the created wound gap in HUVECs monolayer (a); cell numbers in the gap after culturing at different concentrations of Cu^{2+} for 6 h (b); HUVECs migartion after culturing at different concentrations for 6 h (c). 0 μM, 0.01 μM, 0.1 μM, 1 μM, 10 μM, and 100 μM are represented concentrations of Cu^{2+} co-culturing with cells, respectively.

solution, and then dehydrated with a series of gradient alcohol solution (30, 50, 75, 90, 95, and 100 v/v%) for 10 min each. Morphology of dehydrated bacteria were observed by SEM (S-3400, Hitachi, Japan). As for bacterial colony counting method, 400 μL of bacterial solution was fetched from 15 mL centrifugal tubes and diluted 10^4 times with physiological saline solution. Then, 100 μL diluted bacteria solution was transferred to standard agar culture plate (Luria Bertani for *E. coli* and Nutrient Broth NO.2 for *S. aureus*) and spread evenly to re-culture for another 16 h at 37 °C. The images of colony counting were taken by FlourChem M (Protein simple). Antibacterial rate was calculated as follows,

$$\text{Antibacterial rate } (\%) = \frac{A - B}{A} \times 100\%$$

where A is the number of bacterial colonies of S0 and B is the number of bacterial colonies of Cu^{2+} solutions (S1–S11).

2.8. Statistical analysis

Test results were analyzed using GraphPad Prism software and showed as the mean ± standard deviations (SD). Statistical analysis was performed using the one-way analysis of variance (ANOVA) followed by Tukey Kramer Multiple comparison post-test using GraphPad Instant Software (GraphPad Software, Inc., USA) with $p < 0.05$ being considered to be statistically significant.

3. Results and discussion

3.1. Responses of cells

Cell inhibition ratio was a vital indicator to assess the cytotoxicity of biomaterials. Fig. 1 showed cell inhibition ratio curves of Cu^{2+} responding to three kinds of cells including HUVECs (Fig. 1a), MC3T3-E1 (Fig. 1b), and rBMSCs (Fig. 1c). According to Fig. 1a, the results showed that proliferation of HUVECs was promoted when concentration of Cu^{2+} was lower than 222 μM. It was worth noting that cytotoxicity increased sharply when concentration of Cu^{2+} exceeded 222 μM. The half maximal inhibitory concentration (IC_{50}) was about 327.9 μM and the inhibition ratio was approximating to 100% when concentrations of Cu^{2+} rose to 666 μM. According to the Fig. 1b, at a concentration of 10 μM lower, Cu^{2+} is safe for MC3T3-E1 and beneficial for its proliferation. The half maximal inhibitory concentration (IC_{50}) was about 134.6 μM and the inhibition ratio rapidly rose to 100% when concentration of Cu^{2+} ranged from 111 μM to 333 μM. Similar results were reported in other Cu^{2+}-doped materials which also exhibited cytotoxicity with the increase of Cu [41]. According to the Fig. 1c, rBMSCs was very sensitive to Cu^{2+}. It showed cytotoxicity at a very low

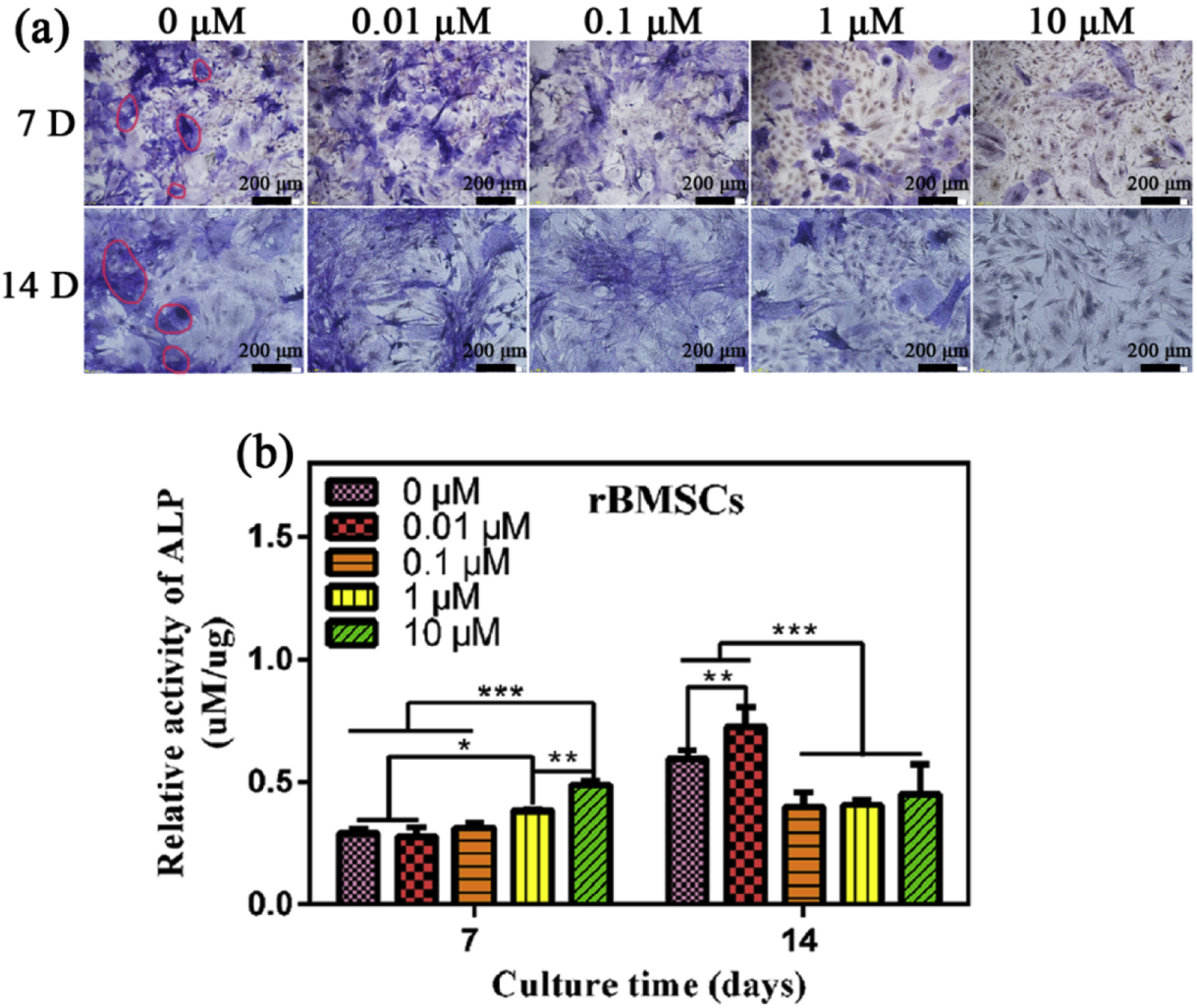

Fig. 3. Qualitative ALP staining images of rBMSCs after culturing 7 days and 14 days (a). 0 μM, 0.01 μM, 0.1 μM, 1 μM, and 10 μM are represented concentrations of Cu^{2+} co-culturing with cells, respectively. Red circle regions are represented as ALP-positive areas; Quantitative osteogenetic-related ALP expression of rBMSC after culturing 7 days and 14 days (b). *$p < 0.05$, **$p < 0.01$, ***$p < 0.001$. (For interpretation of the references to colour in this figure legend, the reader is referred to the web version of this article.)

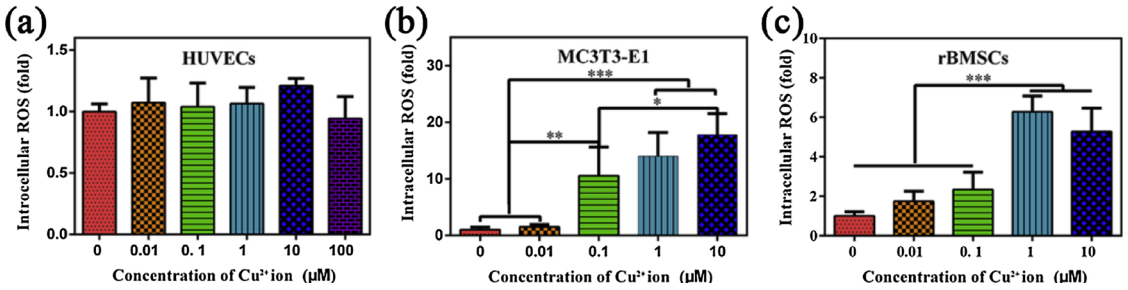

Fig. 4. Intracellular ROS level of HUVECs (a), MC3T3-E1 (b), and rBMSCs (c) after culturing for 1 day.

concentration of Cu^{2+} and IC_{50} was about 0.7 μM. However, the inhibition ratio curve was changed gently with the variation of concentration of Cu^{2+} when compared to HUVECs and MC3T3-E1. It was reported that 10 μM Cu^{2+} inhibited proliferation of rBMSCs [42], which was close to our results. In summary, Cu^{2+} tolerance for these three kinds of cells decreased as follows: HUVECs > MC3T3-E1 > rBMSCs.

Cell migration of endothelial cell should be taken into account for surgical implantations, because it is very important to wound healing. The scratch assay is a useful and low-priced method to measure cell migration *in vitro* [43]. All of the scratch gaps were obviously narrowed down after culturing for 6 h as showed in Fig. 2a and c. It was obviously that high concentrations of Cu^{2+} were beneficial to cell migration compared with low concentrations as showed in Fig. 2b. It was a positive relationship between cell migration and concentrations of Cu^{2+} at low concentrations (0–1 μM). When the concentrations of Cu^{2+} exceeded 1 μM, the effect of Cu^{2+} to cell migration was changed insignificantly.

As an early marker of osteogenic differentiation, ALP activities of rBMSCs were assessed after culturing for 7 and 14 days, respectively. Fig. 3a qualitatively demonstrates ALP staining of rBMSCs incubated with Cu^{2+}-containing culture medium, and ALP-positive rBMSCs are identified by blue staining (red circles). It is obvious that, compared to control (0 μM Cu^{2+}), the number of ALP stained cells was significantly increased in the culture medium containing 0.01 μM Cu^{2+}, remained at the same level incubated with 0.1 and 1 μM Cu^{2+}, and decreased incubated with 10 μM Cu^{2+}. However, the numbers of viable cells gradually decreased with the increasing Cu^{2+} concentrations. For the quantitative results, the ALP activities showed a positive correlation with the rise in concentration of Cu^{2+} at day 7, suggesting that higher concentration of Cu^{2+} could augment the ALP activity of rBMSCs in the earlier days. However, after culturing for 14 days, the trend had clearly changed. The relative ALP activities incubated with high concentrations (0.1 μM, 1 μM, and 10 μM) were significantly decreased compared to those incubated with 0.01 μM Cu^{2+} and control medium. These results demonstrated that copper diminished the proliferation rate of rBMSCs, but increasing their ability to differentiate into the osteogenic lineages, especially in lower concentration.

As mentioned above, results showed that Cu^{2+} had a great influence on the cellular behaviors, and a quite different susceptibility in three kinds of cells was observed. As illustrated in Fig. 1, rBMSCs exhibited higher susceptibility to Cu^{2+} exposure compared to MC3T3-E1 and HUVECs. The different cytotoxic potential of Cu^{2+} in different cells might be correlated with excessive production of reactive oxygen species (ROS) [44]. Many studies revealed that Cu toxicity caused by participating in the formation of ROS modifies the structure and/or function of essential biomolecules [45]. For instance, Pourahmad et al. demonstrated that there is an immediate and rapid increase in ROS production when hepatocytes are incubated with Cu, and the Cu^{2+}-induced cytotoxicity occurs as a result of a mitochondrial 'ROS' formation [46]. In this study, we explored the potential of copper to induce oxidative stress by measuring the ROS levels of different cells. Quantitative data exhibited that copper promoted ROS generation in a dose-dependent manner in rBMSCs and MC3T3-E1, and a sharply increased ROS level was induced at the concentration of 0.1 μM for MC3T3-E1 and 1 μM for rBMSCs (Fig. 4). Comparatively, copper had little effect on ROS production in HUVECs. This may be ascribed to the important role of ROS in angiogenesis in endothelial cells [47]. It has been reported that ROS mediate a number of angiogenic responses and elevated ROS level can induce the expression of angiogenic factors such as vascular endothelial growth factor (VEGF) and angiopoietin-1 (Ang1) [48].

3.2. Antibacterial assay

The Gram-negative *E. coli* and Gram-positive *S. aureus* were used to evaluate antibacterial activities of different concentrations Cu^{2+} solution. Bacterial antibacterial rate curves of *E. coli* and *S. aureus* were presented in Fig. 5. For *E. coli,* it is clear that antibacterial activity was enhanced accompanying with the rise of concentration of Cu^{2+} solution as showed in Fig. 5a. When concentration of Cu^{2+} was lower than 37 μM, it wouldn't show significantly antibacterial activity to *E. coli*. Once the concentration of Cu^{2+} over 37 μM, inhibition ratio suddenly increased and approached to 100% at 111 μM. Fig. 5b showed that the antibacterial rate curve of *S. aureus* which had a similarly trend increasing with the increasing concentrations of Cu^{2+} compared with *E.*

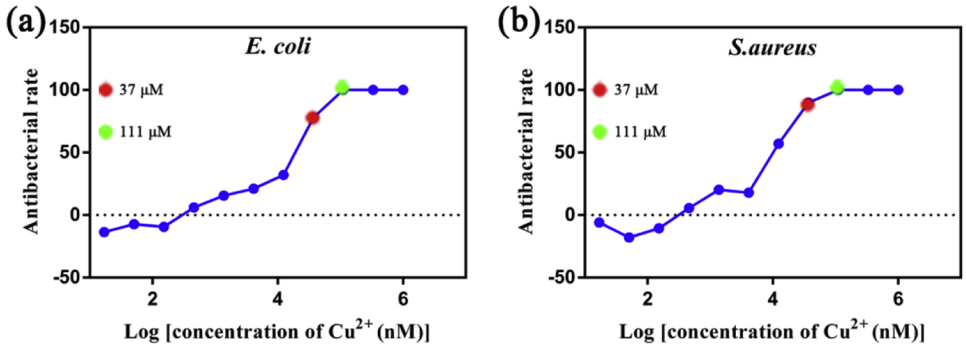

Fig. 5. Antibacterial rate curves of Cu^{2+} responses to bacteria: (a) *E. coli* and (b) *S. aureus.*

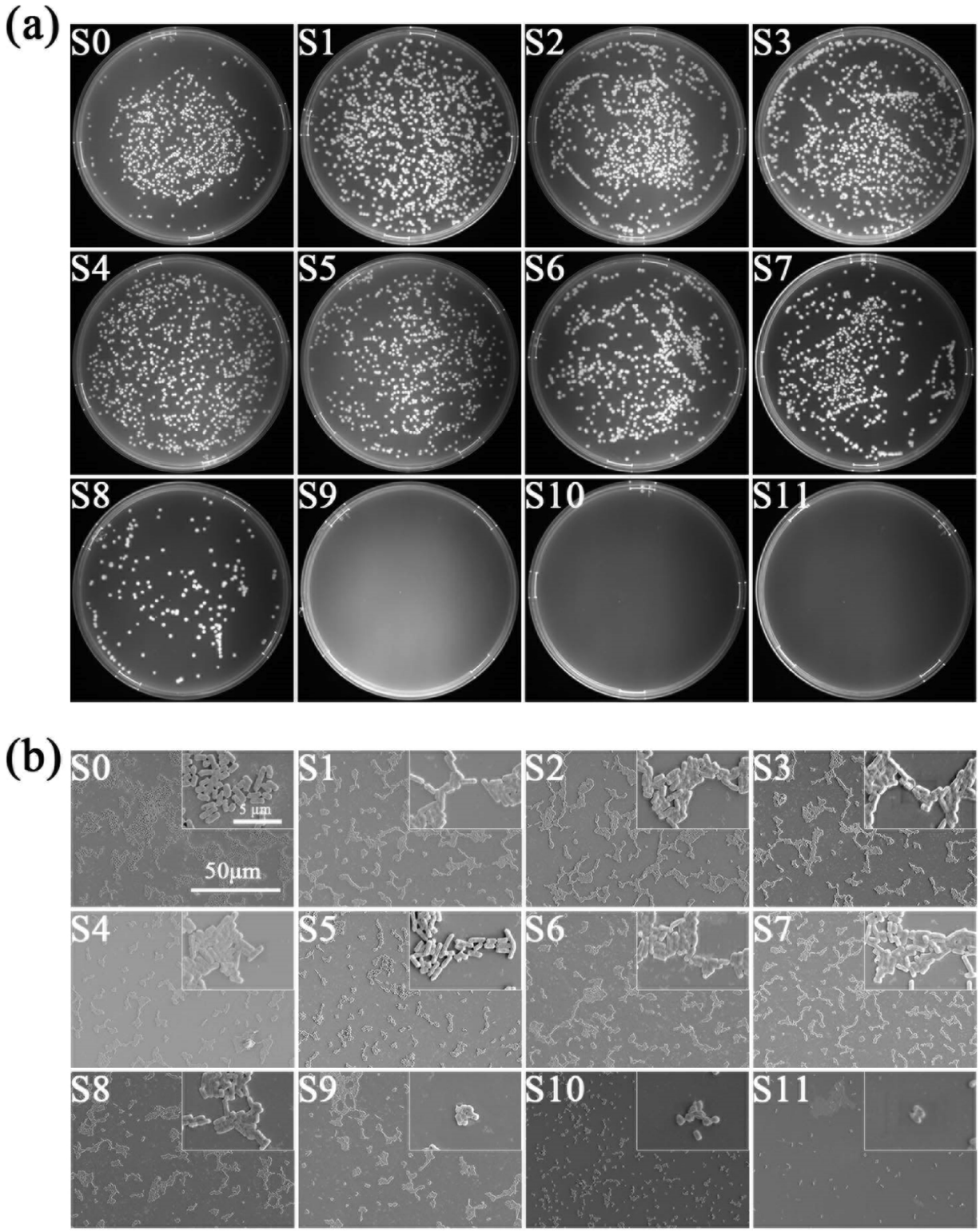

Fig. 6. Bacterial colonies of re-cultivated *E. coli* on agar culture plates (a). SEM morphologies of *E. coli* cultured with different concentrations of Cu^{2+} (b). S0, S1, S2, S3, S4, S5, S6, S7, S8, S9, S10, and S11 were represented as concentrations of Cu^{2+}, 0 μM, 0.017 μM, 0.05 μM, 0.15 μM, 0.45 μM, 1.37 μM, 4.12 μM, 12.34 μM, 37 μM, 111 μM, 333 μM, and 1 mM, respectively.

coli. The antibacterial rate was about 90% at concentration of 37 μM and approached 100% at concentration of 111 μM.

The results of bacterial colonies and SEM morphologies of *E. coli* were presented in Fig. 6. Those results were consistent with the antibacterial rate curves. When the concentrations of Cu^{2+} were lower than 37 μM (S8), bacterial colonies and SEM morphologies of *E. coli* showed it grew well and didn't vary with the concentrations of Cu^{2+} (S0–S7). In contrast, once the concentration of Cu^{2+} over 37 μM (S8), bacterial colonies of *E. coli* decreased sharply. SEM morphologies showed that bacterial numbers were significantly reduced. At the high magnifications, it showed that there were filamentous connections among bacteria at low concentrations, but those filaments vanished with the

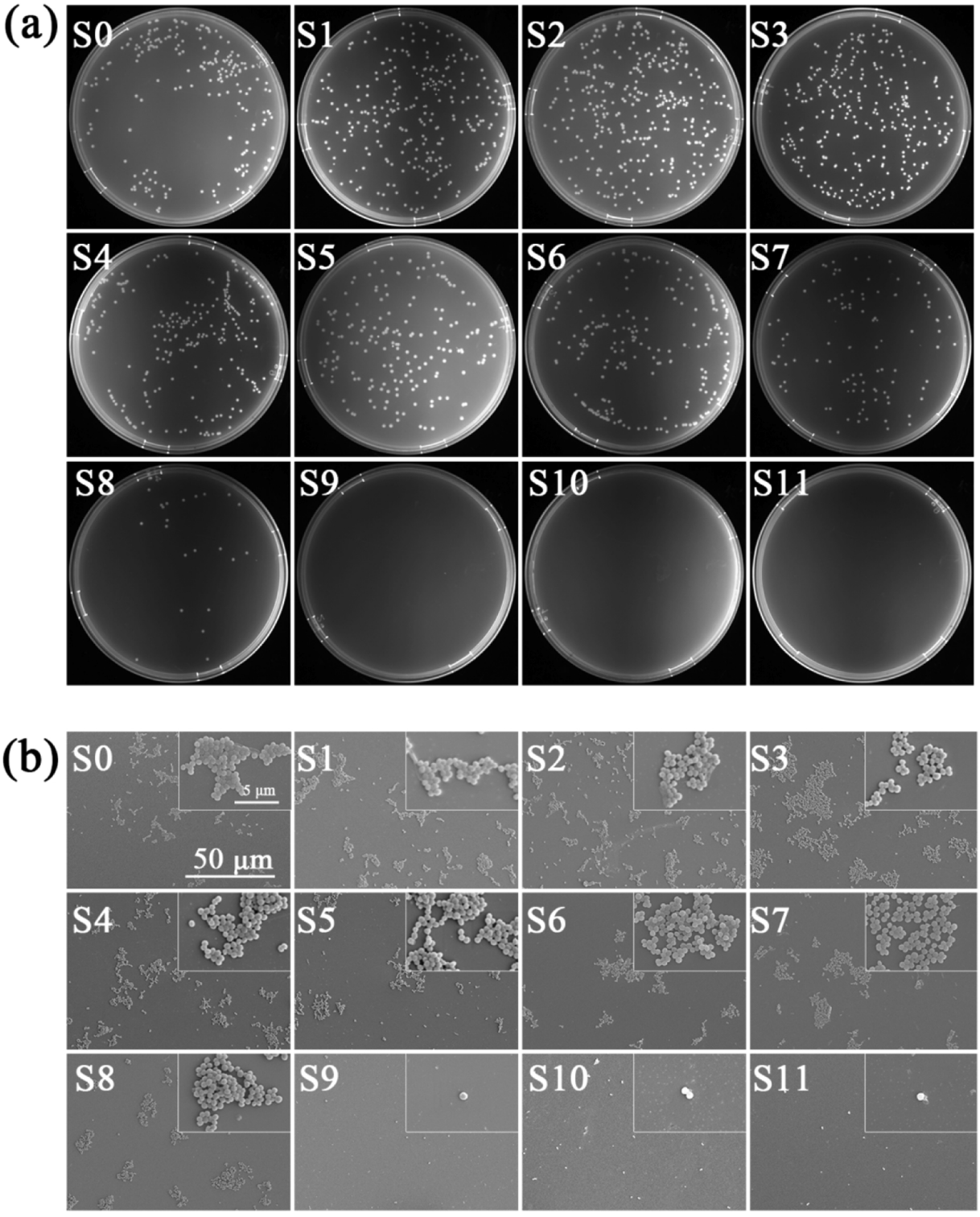

Fig. 7. Bacterial colonies of re-cultivated *S. aureus* on agar culture plates (a). SEM morphologies of *S. aureus* cultured with different concentrations of Cu^{2+} (b). S0, S1, S2, S3, S4, S5, S6, S7, S8, S9, S10, and S11 were represented as concentrations of Cu^{2+}, 0 μM, 0.017 μM, 0.05 μM, 0.15 μM, 0.45 μM, 1.37 μM, 4.12 μM, 12.34 μM, 37 μM, 111 μM, 333 μM, and 1 mM, respectively.

increase of concentrations of Cu^{2+}. Particularly, the bacterial membranes were deformed badly when the concentrations of Cu^{2+} exceeded 111 μM. The results of colony and SEM morphologies of *S. aureus* were shown in Fig. 7. Those results showed similar trend as *E. coli*.

As mentioned above, our results showed that there was a threshold concentration for Cu^{2+} to perform antibacterial activity. Parmar et al. provided us with a mathematical model to analysis copper uptake kinetics which showed that bacteria would lose controllability of copper once beyond the threshold concentration [49]. It could also explain our results. It wouldn't show antibacterial properties when concentrations of Cu^{2+} below the critical value, because bacteria are good at control of copper levels. On the contrary, the concentration of Cu^{2+} exceeds critical value resulted that bacteria lose control of copper levels. The antibacterial activity would be enhanced very soon.

From the above results, combined analysis of cell and bacterial studies identified a threshold concentration at which the material shows outstanding antibacterial properties without significantly affecting the viabilities of bone cells and HUVECs. This key outcome sets Cu doping as a promising strategy for biomaterials design and encourages further investigation on similar systems toward the development of multifunctional biomaterials.

4. Conclusion

In this study, we discussed different doses of Cu^{2+} responding to three kinds of cells (HUVECs, MC3T3-E1, and rBMSCs) and two kinds of bacteria (*E. coli* and *S. aureus*) *in vitro*. According to analyses mentioned above, differential toxicity of Cu^{2+} in different cells was observed, and their susceptibility increased as follows: HUVECs (IC_{50} = 327.9 μM) > MC3T3-E1 (IC_{50} = 134.6 μM) > rBMSCs (IC_{50} = 0.7 μM). Moreover, there was also a threshold concentration (37 μM) of copper to exhibit excellent antibacterial activities against *E. coli* and *S. aureus*. Therefore, the results performed on cells and bacteria yields good osteogenic, angiogenic and antibacterial activities.

Acknowledgments

Financial support from the National Key Research and Development Program of China (2016YFC1100600, 2016YFC1100604), National Natural Science Foundation of China (31570973, 31870944), National Natural Science Foundation for Distinguished Young Scholars of China (51525207), Science and Technology Commission of Shanghai Municipality (18410760600), International Partnership Program of Chinese Academy of Sciences (GJHZ1850), Science Foundation for Youth Scholar of State Key Laboratory of High Performance Ceramics and Superfine Microstructures (SKL201606) are acknowledged.

References

[1] K. Yuan, K.C. Chen, Y.J. Chan, C.C. Tsai, H.H. Chen, C.C. Shih, Dental implant failure associated with bacterial infection and long-term bisphosphonate usage: a case report, Implant Dent. 21 (1) (2012) 3–7, https://doi.org/10.1097/ID.0b013e3182425c62.

[2] X. Liu, P. Chu, C. Ding, Surface modification of titanium, titanium alloys, and related materials for biomedical applications, Mater. Sci. Eng. R: Rep. 47 (3–4) (2004) 49–121, https://doi.org/10.1016/j.mser.2004.11.001.

[3] B.D. Ratner, A.S. Hoffman, F.J. Schoen, J.E. Lemons, Front matter, Biomaterials Science (third Edition), Academic Press, 2013, https://doi.org/10.1016/B978-0-08-087780-8.00148-0.

[4] H. Zhu, G. Jin, H. Cao, Y. Qiao, X. Liu, Influence of implantation voltage on the biological properties of zinc-implanted titanium, Surf. Coat. Technol. 312 (2017) 75–80, https://doi.org/10.1016/j.surfcoat.2016.09.054.

[5] A.R. Deokar, Y. Shalom, I. Perelshtein, N. Perkas, A. Gedanken, E. Banin, A topical antibacterial ointment made of zn-doped copper oxide nanocomposite, J. Nanopart. Res. 18 (8) (2016) 218, https://doi.org/10.1007/s11051-016-3534-7.

[6] M. Cheng, Y. Qiao, Q. Wang, G. Jin, H. Qin, Y. Zhao, X. Peng, X. Zhang, X. Liu, Calcium plasma implanted titanium surface with hierarchical microstructure for improving the bone formation, ACS Appl. Mater. Interfaces 7 (23) (2015) 13053–13061, https://doi.org/10.1021/acsami.5b03209.

[7] T. Lu, S. Qian, F. Meng, C. Ning, X. Liu, Enhanced osteogenic activity of poly ether ether ketone using calcium plasma immersion ion implantation, Colloids Surf. B: Biointerfaces 142 (2016) 192–198, https://doi.org/10.1016/j.colsurfb.2016.02.056.

[8] L. Yu, Y. Tian, Y. Qiao, X. Liu, Mn-containing titanium surface with favorable osteogenic and antimicrobial functions synthesized by PIII&D, Colloids Surf. B: Biointerfaces 152 (2017) 376–384, https://doi.org/10.1016/j.colsurfb.2017.01.047.

[9] H. Hu, Y. Tang, L. Pang, C. Lin, W. Huang, D. Wang, W. Jia, Angiogenesis and full-thickness wound healing efficiency of a copper-doped borate bioactive glass/poly (lactic- co-glycolic acid) dressing loaded with vitamin e in vivo and in vitro, ACS Appl. Mater. Interfaces 10 (27) (2018) 22939–22950, https://doi.org/10.1021/acsami.8b04903.

[10] A. Bari, N. Bloise, S. Fiorilli, G. Novajra, M. Vallet-Regi, G. Bruni, A. Torres-Pardo, J.M. Gonzalez-Calbet, L. Visai, C. Vitale-Brovarone, Copper-containing mesoporous bioactive glass nanoparticles as multifunctional agent for bone regeneration, Acta Biomater. 55 (2017) 493–504, https://doi.org/10.1016/j.actbio.2017.04.012.

[11] M.X. Zong, L. Bai, Y.L. Liu, X. Wang, X.Y. Zhang, X.B. Huang, R.Q. Hang, B. Tang, Antibacterial ability and angiogenic activity of Cu-Ti-O nanotube arrays, Mater. Sci. Eng. C: Mater. Biol. Appl. 71 (2017) 93–99, https://doi.org/10.1016/j.msec.2016.09.077.

[12] W.L. Yu, T.W. Sun, Z.Y. Ding, C. Qi, H.K. Zhao, F. Chen, Z.M. Shi, Y.J. Zhu, D.Y. Chen, Y.H. He, Copper-doped mesoporous hydroxyapatite microspheres synthesized by a microwave-hydrothermal method using creatine phosphate as an organic phosphorus source: application in drug delivery and enhanced bone regeneration, J. Mater. Chem. B 5 (5) (2017) 1039–1052, https://doi.org/10.1039/c6tb02747d.

[13] E. Schipani, C. Maes, G. Carmeliet, G.L. Semenza, Regulation of osteogenesis-angiogenesis coupling by HIFs and VEGF, J. Bone Miner. Res. 24 (8) (2009) 1347–1353, https://doi.org/10.1359/Jbmr.090602.

[14] A.P. Kusumbe, S.K. Ramasamy, R.H. Adams, Coupling of angiogenesis and osteogenesis by a specific vessel subtype in bone, Nature 513 (7519) (2014) 323, https://doi.org/10.1038/nature13720.

[15] A. Hoppe, N.S. Guldal, A.R. Boccaccini, A review of the biological response to ionic dissolution products from bioactive glasses and glass-ceramics, Biomaterials 32 (11) (2011) 2757–2772, https://doi.org/10.1016/j.biomaterials.2011.01.004.

[16] F. Martin, T. Linden, D.M. Katschinski, F. Oehme, I. Flamme, C.K. Mukhopadhyay, K. Eckhardt, J. Troger, S. Barth, G. Camenisch, R.H. Wenger, Copper-dependent activation of hypoxia-inducible factor (HIF)-1: implications for ceruloplasmin regulation, Blood 105 (12) (2005) 4613–4619, https://doi.org/10.1182/blood-2004-10-3980.

[17] C.K. Sen, S. Khanna, M. Venojarvi, P. Trikha, E.C. Ellison, T.K. Hunt, S. Roy, Copper-induced vascular endothelial growth factor expression and wound healing, Am. J. Physiol. Heart Circ. Physiol. 282 (5) (2002) H1821–7, https://doi.org/10.1152/ajpheart.01015.2001.

[18] D.A. Towler, Vascular biology and bone formation: hints from HIF, J. Clin. Invest. 117 (6) (2007) 1477–1480, https://doi.org/10.1172/Jci32518.

[19] J.C. Zhang, J.A. Huang, S.J. Xu, K. Wang, S.F. Yu, Effects of Cu2+ and pH on osteoclastic bone resorption in vitro, Prog. Nat. Sci.-Mater. 13 (4) (2003) 266, https://doi.org/10.1080/10020070312331343510.

[20] J.P. Rodriguez, S. Rios, M. Gonzalez, Modulation of the proliferation and differentiation of human mesenchymal stem cells by copper, J. Cell. Biochem. 85 (1) (2002) 92–100, https://doi.org/10.1002/jcb.10111.

[21] J.O. Noyce, H. Michels, C.W. Keevil, Potential use of copper surfaces to reduce survival of epidemic meticillin-resistant Staphylococcus aureus in the healthcare environment, J. Hosp. Infect. 63 (3) (2006) 289–297, https://doi.org/10.1016/j.jhin.2005.12.008.

[22] H.W. Chai, L. Guo, X.T. Wang, Y.P. Fu, J.L. Guan, L.L. Tan, L. Ren, K. Yang, Antibacterial effect of 317l stainless steel contained copper in prevention of implant-related infection in vitro and in vivo, J. Mater. Sci.—Mater. Med. 22 (11) (2011) 2525–2535, https://doi.org/10.1007/s10856-011-4427-z.

[23] T. Tian, C.T. Wu, J. Chang, Preparation and in vitro osteogenic, angiogenic and antibacterial properties of cuprorivaite (CaCuSi4O10, Cup) bioceramics, RSC Adv. 6 (51) (2016) 45840–45849, https://doi.org/10.1039/c6ra08145b.

[24] L. Peng, C. Ning, D. Ding, X. Liu, Mechanical properties and protein adsorption of Ca5(PO4)2SiO4 bioceramics sintered from solid state reaction derived powders, J. Biomater. Tissue Eng. 5 (2) (2015) 157–163, https://doi.org/10.1166/jbt.2015.1292.

[25] C. Wang, S. Wang, K. Li, Y. Ju, J. Li, Y. Zhang, J. Li, X. Liu, X. Shi, Q. Zhao, Preparation of laponite bioceramics for potential bone tissue engineering applications, PLoS One 9 (6) (2014) e99585, https://doi.org/10.1371/journal.pone.0099585.

[26] J. Li, D. Zhai, F. Lv, Q. Yu, H. Ma, J. Yin, Z. Yi, M. Liu, J. Chang, C. Wu, Preparation of copper-containing bioactive glass/eggshell membrane nanocomposites for improving angiogenesis, antibacterial activity and wound healing, Acta Biomater. 36 (2016) 254–266, https://doi.org/10.1016/j.actbio.2016.03.011.

[27] Y. Lin, W. Xiao, B.S. Bal, M.N. Rahaman, Effect of copper-doped silicate 13-93 bioactive glass scaffolds on the response of MC3T3-E1 cells in vitro and on bone regeneration and angiogenesis in rat calvarial defects in vivo, Mater. Sci. Eng. C: Mater. Biol. Appl. 67 (2016) 440–452, https://doi.org/10.1016/j.msec.2016.05.073.

[28] J. Xiao, S. Chen, J. Yi, H.F. Zhang, G.A. Ameer, A cooperative copper metal-organic framework-hydrogel system improves wound healing in diabetes, Adv. Funct. Mater. 27 (1) (2017) 1604872, https://doi.org/10.1002/adfm.201604872.

[29] R. Liu, K. Memarzadeh, B. Chang, Y.M. Zhang, Z. Ma, R.P. Allaker, L. Ren, K. Yang, Antibacterial effect of copper-bearing titanium alloy (Ti-Cu) against streptococcus mutans and Porphyromonas gingivalis, Sci. Rep. 6 (2016) 29985, https://doi.org/10.1038/srep29985.

[30] L. Yu, G.D. Jin, L.P. Ouyang, D.H. Wang, Y.Q. Qiao, X.Y. Liu, Antibacterial activity, osteogenic and angiogenic behaviors of copper-bearing titanium synthesized by PIII &D, J. Mater. Chem. B 4 (7) (2016) 1296–1309, https://doi.org/10.1039/c5tb02300a.

[31] Q.J. Wu, J.H. Li, W.J. Zhang, H.X. Qian, W.J. She, H.Y. Pan, J. Wen, X.L. Zhang, X.Y. Liu, X.Q. Jiang, Antibacterial property, angiogenic and osteogenic activity of Cu-incorporated TiO2 coating, J. Mater. Chem. B 2 (39) (2014) 6738–6748, https://doi.org/10.1039/c4tb00923a.

[32] F. Hempel, B. Finke, C. Zietz, R. Bader, K.D. Weltmann, M. Polak, Antimicrobial surface modification of titanium substrates by means of plasma immersion ion implantation and deposition of copper, Surf. Coat. Technol. 256 (2014) 52–58, https://doi.org/10.1016/j.surfcoat.2014.01.027.

[33] R. Liu, Y. Tang, L. Zeng, Y. Zhao, Z. Ma, Z. Sun, L. Xiang, L. Ren, K. Yang, In vitro and in vivo studies of anti-bacterial copper-bearing titanium alloy for dental application, Dent. Mater. 34 (8) (2018) 1112–1126, https://doi.org/10.1016/j.dental.2018.04.007.

[34] U. Walschus, A. Hoene, M. Patrzyk, S. Lucke, B. Finke, M. Polak, G. Lukowski, R. Bader, C. Zietz, A. Podbielski, J.B. Nebe, M. Schlosser, A cell-adhesive plasma

polymerized allylamine coating reduces the in vivo inflammatory response induced by Ti6Al4V modified with plasma immersion ion implantation of copper, J. Funct. Biomater. 8 (3) (2017) 30, https://doi.org/10.3390/jfb8030030.
[35] C. Liu, X.K. Fu, H.B. Pan, P. Wan, L. Wang, L.L. Tan, K.H. Wang, Y. Zhao, K. Yang, P.K. Chu, Biodegradable Mg-Cu alloys with enhanced osteogenesis, angiogenesis, and long-lasting antibacterial effects, Sci. Rep. 6 (2016), https://doi.org/10.1038/srep27374.
[36] M.C. Linder, M. HazeghAzam, Copper biochemistry and molecular biology, Am. J. Clin. Nutr. 63 (5) (1996) 797–811.
[37] E.D. Harris, Copper homeostasis: the role of cellular transporters, Nutr. Rev. 59 (9) (2001) 281–285.
[38] J.F.B. Mercer, The molecular basis of copper-transport diseases, Trends Mol. Med. 7 (2) (2001) 64–69, https://doi.org/10.1016/S1471-4914(01)01920-7.
[39] X. Wang, F. Cheng, J. Liu, J.H. Smatt, D. Gepperth, M. Lastusaari, C. Xu, L. Hupa, Biocomposites of copper-containing mesoporous bioactive glass and nanofibrillated cellulose: biocompatibility and angiogenic promotion in chronic wound healing application, Acta Biomater. 46 (2016) 286–298, https://doi.org/10.1016/j.actbio.2016.09.021.
[40] C.R. Guo, L. Li, S.S. Li, Y.P. Wang, X.X. Yu, Preparation, characterization, bioactivity and degradation behavior in vitro of copper-doped calcium polyphosphate as a candidate material for bone tissue engineering, RSC Adv. 7 (67) (2017) 42614–42626, https://doi.org/10.1039/c7ra06159e.
[41] Y.N. Lin, W. Xiao, B.S. Bal, M.N. Rahaman, Effect of copper-doped silicate 13-93 bioactive glass scaffolds on the response of MC3T3-E1 cells in vitro and on bone regeneration and angiogenesis in rat calvarial defects in vivo, Mater. Sci. Eng. C: Mater. Biol. Appl. 67 (2016) 440–452, https://doi.org/10.1016/j.msec.2016.05.073.
[42] S. Li, M. Wang, X. Chen, S.F. Li, J. Li-Ling, H.Q. Xie, Inhibition of osteogenic differentiation of mesenchymal stem cells by copper supplementation, Cell Proliferat. 47 (1) (2014) 81–90, https://doi.org/10.1111/Cpr.12083.
[43] C.C. Liang, A.Y. Park, J.L. Guan, In vitro scratch assay: a convenient and inexpensive method for analysis of cell migration in vitro, Nat. Protoc. 2 (2) (2007) 329–333, https://doi.org/10.1038/nprot.2007.30.
[44] L.M. Gaetke, C.K. Chow, Copper toxicity, oxidative stress, and antioxidant nutrients, Toxicology 189 (1–2) (2003) 147–163, https://doi.org/10.1016/s0300-483x(03)00159-8.
[45] S.J. Lippard, Biochemistry - free copper ions in the cell? Science 284 (5415) (1999) 748–749, https://doi.org/10.1126/science.284.5415.748.
[46] J. Pourahmad, P.J. O'Brien, A comparison of hepatocyte cytotoxic mechanisms for Cu^{2+} and Cd^{2+}, Toxicology 143 (3) (2000) 263–273, https://doi.org/10.1016/S0300-483x(99)00178-X.
[47] Y. Taniyama, K.K. Griendling, Reactive oxygen species in the vasculature - molecular and cellular mechanisms, Hypertension 42 (6) (2003) 1075–1081, https://doi.org/10.1161/01.Hyp.0000100443.09293.4f.
[48] D.Q. Guo, Q.Y. Wang, C. Li, Y. Wang, X. Chen, Vegf stimulated the angiogenesis by promoting the mitochondrial functions, Oncotarget 8 (44) (2017) 77020–77027, https://doi.org/10.18632/oncotarget.20331.
[49] J.H. Parmar, J. Quintana, D. Ramirez, R. Laubenbacher, J.M. Arguello, P. Mendes, An important role for periplasmic storage in pseudomonas aeruginosa copper homeostasis revealed by a combined experimental and computational modeling study, Mol. Microbiol. 110 (3) (2018) 357–369, https://doi.org/10.1111/mmi.14086.